Parity violation in deuteron photodisintegration

M. Fujiwara[1,2] and A. I. Titov[1,3]

[1]*Advanced Science Research Center, Japan Atomic Energy Research Institute, Tokai, Ibaraki 319-1195, Japan*

[2]*Research Center of Nuclear Physics, Osaka University, Ibaraki, Osaka 567-0047, Japan*

[3]*Bogoliubov Laboratory of Theoretical Physics, JINR, Dubna 141980, Russia*

(Received 10 October 2003; published 30 June 2004)

We analyze the energy dependence for two parity-nonconserving (PNC) asymmetries in the reaction $\gamma D \to np$ in the near-threshold region. First, we analyze the asymmetry in the reaction between a circularly polarized photon beam and an unpolarized deuteron. Second, we examine the reaction between an unpolarized photon and a polarized deuteron. We find that the two asymmetries have quite different energy dependence, and that the shapes are sensitive to the PNC meson-exchange coupling constants. The constraints for the PNC coupling constants and how to obtain them from future experiments are discussed.

DOI: 10.1103/PhysRevC.69.065503 PACS number(s): 11.30.Er, 13.75.Cs, 25.40.Lw

I. INTRODUCTION

For more than 40 years, the parity nonconservation (PNC) in nuclear processes attracts attention as a unique tool for studying the strangeness conserving ($\Delta S=0$) weak nucleon-nucleon interaction defined by nontrivial interplay of the weak quark-quark interaction and the QCD dynamics of composite hadrons at short distances [1,2]. Most of the present theoretical studies of parity nonconservation in nuclear processes are based on the finite-range π-, ω-, and ρ-meson exchange potential of Desplanques, Donoghue, and Holstein (DDH) [3]. Using the symmetry consideration and the constituent quark model, DDH found the "reasonable range" and the "best values" of the PNC meson-nucleon coupling constants. Their predictions are related to the theory of the weak interaction. Thus, the best values of the πNN coupling obtained using the Cabibbo and Weinberg-Salam models correspond to $h_\pi \simeq 0.2$ and 4.6 (in units of 10^{-7}), respectively. The predictions for the vector meson-nucleon weak coupling constants are also "theory dependent," but this dependence is not so strong. In case of the charge-current theory, the transition $u \to s$ responsible for the πNN interaction is suppressed by $\tan^2\theta_C \simeq 0.05$ (θ_C is the Cabibbo angle) as compared with the other transitions. This results in strong reduction of h_π. The neutral-current theory is free from this suppression which leads to a large value of h_π. The value of h_π depends also on the nonperturbative QCD dynamics of interacting mesons and baryons. The predictions based on the Skyrmion model [4], the QCD sum rule [5], the soft-pion approximation [6], and the quark model with the Δ degrees of freedom [7] give the value of $h_\pi = (0.8-3) \times 10^{-7}$ which is in the reasonable range of the DDH prediction (in the Weinberg-Salam model), being smaller than the corresponding best value (see Ref. [8] for the review of the estimations).

Analysis of the available data from nuclear PNC experiments suggests that the isoscalar PNC nuclear forces dominated by the ρ- and ω-meson exchange are comparable with the DDH best values, whereas the isovector interaction dominated by the π-meson exchange is weak by a factor of 3 [2]. For example, the measurement of the circular polarization of the photons emitted from ^{18}F results in the constraint of $0 \leqslant h_\pi \leqslant 1.8(\times 10^{-7})$ [10]. However, this constraint is in disagreement with the recent analysis of the ^{133}Cs anapole moment [11,12] performed in Refs. [8,13]. Quite different theoretical approaches result in similar conclusions: for adequate description of the data on the anapole moment, one needs to use h_π which is a factor of about 2 greater than the DDH best value $h_\pi^{\rm best} \simeq 4.6 \times 10^{-7}$. These experiments mentioned above call for the new measurements and theoretical studies to resolve subsisting inconsistencies.

The studies of the PNC transitions in the nucleon-nucleon are very attractive because the two-nucleon wave functions are known reasonably well. Together with the PNC measurements in $\vec{p}p$ scattering [14,15], the reactions $\gamma D \rightleftarrows np$ are particularly important. Up to now, great efforts have been devoted to analyzing the thermal neutron capture by proton in the reactions with unpolarized and polarized neutrons. In this first case, the circular polarization P_γ of emitted 2.23 MeV photons is analyzed. The experimental value $|P_\gamma| = (18 \pm 18) \times 10^{-8}$ [16] is consistent with the theoretical estimations $|P_\gamma| = (1.8-5.6) \times 10^{-8}$ [17–19]. But poor accuracy does not allow us to obtain any definite conclusion about the strength of the PNC forces. In the second case, the subject of study is the spatial asymmetry A_γ of emitted photons. The experimental value of $A_\gamma = (6 \pm 21) \times 10^{-8}$ [20] is again too crude to check the theoretical predictions of $A_\gamma \sim 5 \times 10^{-8}$, (see, e.g., Ref. [21] for reference and quotations). At present, a new PNC-asymmetry measurement for the radiative neutron-proton capture is in preparation at LANSCE [22] in order to reduce the experimental error of A_γ.

Different aspects of parity nonconservation in deuteron electrodisintegration were analyzed in Refs. [23–25]. However, the nuclear PNC effect in this reaction is found to be insignificant compared to the contribution of the γ–Z-boson interference of the individual nucleons [25].

With the advent of the high-intensity polarized photon beams, investigation of PNC effects in the $\gamma D \to np$ reaction becomes very important [26], because one can expect to obtain complementary information on the PNC interaction. In fact, the study of the PNC asymmetries as a function of the photon energy (contrary to the radiative np capture, where the photon energy is fixed: $E_\gamma \simeq 2.23$ MeV) allows us to ob-

0556-2813/2004/69(6)/065503(10)/$22.50

tain additional information which might reduce the ambiguity induced by uncertainties of the parity-conserving NN forces at short distances. Thus, for example, the constraints on the PNC meson-exchange coupling constants are usually obtained from the data compilation from various experiments [8]. This analysis includes a model-dependent estimation of the PNC matrix elements in quite different observables such as two- and few-body systems, and light and heavy nuclei with their own assumptions and approximations. The energy dependent asymmetries in the $\gamma D \to pn$ reaction allow us to give the similar constraints using only one simplest nuclear system.

In this paper, we discuss two PNC asymmetries. One is the asymmetry A_{RL} in deuteron disintegration in the reaction between the circularly polarized photon and an unpolarized deuteron. This asymmetry is mainly defined by the $\Delta I = 0,2$ PNC interaction and is equal to P_γ at $E_\gamma \simeq E_{\rm thr}$, where $E_{\rm thr}$ is the threshold energy. The second one is the deuteron spin asymmetry A_D in the reaction between an unpolarized photon and a polarized deuteron (polarized along-opposite to the beam direction). It depends also on the isovector $\Delta I = 1$ PNC interaction, and therefore may be used for examining h_π. The A_{RL} asymmetry was analyzed previously in Refs. [27–29]. In Refs. [27,28], the calculation has been done only with repulsive hard-core NN potentials which seem to be obsolete compared to the more sophisticated realistic potentials with a soft repulsive core. Energy dependence of A_{RL} in the region $E_\gamma - E_{\rm thr} \sim 0.5-5$ MeV was skipped. In Ref. [27], the contribution of the PNC πNN transitions were completely ignored. On the other hand, they were included in Ref. [28], and the extraordinarily big contribution of the weak πNN transitions to A_{RL} at $E_\gamma - E_{\rm thr} = 1-30$ MeV has been reported. This result was used by other authors (e.g., Refs. [6,31]) to discuss a possibility for extracting h_π from the A_{RL} asymmetry.

However, in Ref. [29], it is shown that the consistent description of all transitions defined by the spin-conserving $\Delta I = 1$ interaction results in the mutual cancellation which is a disadvantage of using A_{RL} as a tool for studying the weak πNN transition [30]. In Ref. [29], the PNC asymmetry is calculated on the basis of zero-range approximation where the short-range behavior of the proton-neutron wave functions is modified phenomenologically, and therefore this result may be considered as a raw qualitative estimation. The PNC asymmetry A_D is analyzed in Ref. [32] in the framework of the same model as given in Ref. [29] and therefore its result remains at very qualitative level.

In our study, we use two realistic NN potentials. One is the Paris potential [33,34] with a soft repulsive core at short distances and another is the Hamada-Johnston (HJ) potential [35] with a hard repulsive core. The long-range meson-exchange part of the NN interaction in these potentials coincides, and the difference appears at short distances. Our results with the Paris potential may be useful as a prediction for possible future experiments, because the Paris potential was designed specially for proper description of the short-range phenomena. The results with the HJ potential are rather illustrative, and we show them in order to link our calculation with the previous works and to show explicitly the effect of the short-range correlation as an example of the extreme hard repulsion.

In calculations of the PNC asymmetries, the usage of models motivated by QCD (e.g., the effective chiral perturbation model (ChPT) [36,37]) seems to be interesting and important. In the present status, the ChPT is, however, useful only for the processes dominated by the long-range $\Delta I = 1$ PNC forces (such as A_γ asymmetry [36]), and it cannot be applied to the considered case where the short-range $\Delta I = 0,2$ transitions are important. Therefore, we perform the present calculation only in the framework of the potential description.

This paper is organized as follows. In Sec. II, we define observables for the regular $M1$ and $E1$ transitions. The formula for the PNC interactions and expressions for the odd-parity admixtures are given in Sec. III. In Sec. IV, we discuss the results and report some predictions for the future experiments. The summary is given in Sec. V.

II. REGULAR TRANSITIONS

Near the threshold with $E_\gamma \leqslant 10$ MeV, the deuteron disintegration $\gamma D \to np$ is dominated by the $M1$ transition $D \to {}^1S_0$ and the $E1$ transition $D \to {}^3P_J$. The amplitudes of these $M1$ and $E1$ transitions read

$$T_\lambda(M1) = \frac{\pm ie\sqrt{k}}{2M} \int d\mathbf{r}\, \psi_f^*(\mu_s \mathbf{S} + \mu_v \boldsymbol{\Sigma} + \mathbf{l}_p)[\mathbf{n} \times \boldsymbol{\varepsilon}_\lambda]\psi_i, \tag{1}$$

$$T_\lambda(E1) = \frac{\pm ie\sqrt{k}}{2} \int d\mathbf{r}\, \psi_f^* \mathbf{r} \boldsymbol{\varepsilon}_\lambda \psi_i, \tag{2}$$

where $\mathbf{k} = \mathbf{n}k$ is the photon momentum, $\boldsymbol{\varepsilon}_\lambda$ is the photon polarization vector, λ is the photon helicity, M is the nucleon mass, $\mu_s = \mu_p + \mu_n = 0.88$, and $\mu_v = \mu_p - \mu_n = 4.71$ are the isoscalar and isovector nucleon magnetic moments, respectively; e is the electric charge, $\alpha = e^2/4\pi = 1/137$, $\mathbf{r}$ is the proton-neutron relative coordinate, $\mathbf{r} = \mathbf{r}_p - \mathbf{r}_n$, $\mathbf{l}_p$ is the proton orbital momentum, $\mathbf{l}_p = -i\mathbf{r}_p \times \boldsymbol{\nabla}_p = -i\mathbf{r} \times \boldsymbol{\nabla}/2 = \mathbf{l}/2$, ψ_i and ψ_f are the proton-neutron wave functions in the initial and final states, defined in the obvious standard notations as

$$\psi_i = \sum_{l\mu\sigma} \langle l\mu 1\sigma | 1M_i \rangle Y_{l\mu}(\hat{\mathbf{r}}) \chi_{1M_i} \frac{u_l(r)}{r},$$

$$\psi_f = 4\pi \sum_{ls\mu\sigma} \langle l\mu s\sigma | JM_f \rangle Y^*_{l\mu}(\hat{\mathbf{p}}) Y_{l\mu}(\hat{\mathbf{r}}) \chi_{s\sigma} \frac{u({}^{2S+1}K_J{:}pr)}{pr}, \tag{3}$$

where $u_0(r) = u(r)$ and $u_2(r) = w(r)$ are the radial deuteron s and d waves, respectively, and $u({}^{2S+1}K_J{:}pr)$ $(K = S, P, \ldots)$ is the radial continuum wave function. The spin operators $\mathbf{S}$ and $\boldsymbol{\Sigma}$ in Eq. (1) are defined as

$$\mathbf{S} = \tfrac{1}{2}(\boldsymbol{\sigma}_p + \boldsymbol{\sigma}_n), \quad \boldsymbol{\Sigma} = \tfrac{1}{2}(\boldsymbol{\sigma}_p - \boldsymbol{\sigma}_n). \tag{4}$$

The upper and lower signs in Eqs. (1) and (2) correspond to the photon absorption or emission, respectively [21].

In the following consideration, the regular and PNC transitions from the deuteron bound state (with the radial wave function u_D) to the np ^3P_J scattering states (with the corresponding radial wave function u_J) will appear. Our analysis shows that these radial integrals at considered energies are not sensitive to J. Therefore, we can use the "degenerated" approximation, in which u_J is calculated with the central forces. The reason for weak sensitivity of the radial integrals to J is that the dominant contribution to the radial integrals comes from relatively large distances, where $u_{0,1,2}$ are close to each other because the phase shifts for different states at $E_\gamma < 10$ MeV are rather small: $|\delta_J| < 4$ degrees. Small distances at $r < 0.5$ fm, where u_J are really different, do not contribute to the integral because u_J are small, and because of strong suppression from $u_D(r)$ [or $ru_D(r)$]. Direct numerical calculation shows that at $E_\gamma \lesssim 10$ MeV, the validity of this approximation is better than 4–5 %, which is quite reasonable. This approximation allows us to express the corresponding matrix elements in a very transparent form useful for qualitative analysis. But this approximation cannot be used for calculation of the odd parity admixtures. In this case, the spin-orbital and tensor parts of the NN potentials have to be taken properly into account.

The regular $M1$ and $E1$ transition amplitudes expressed through the radial proton-neutron wave functions have the following forms:

$$T_\lambda(M1) = -\lambda N \frac{\mu_v}{M} I_M^0 \delta_{-\lambda M_i}, \quad I_M^0 = \int u^*(^1S_0{:}pr)u(r)dr, \tag{5}$$

$$T_\lambda(E1) = iN\sqrt{\frac{4\pi}{3}} \sum_{\mu,\sigma M_f} \langle 1\mu 1\sigma | JM_f\rangle Y^*_{1\mu}(\hat{\mathbf{p}})[\delta_{\mu\lambda}\delta_{\sigma M_i} I_E^0 - \sqrt{2}\langle 2m1\sigma|1M_i\rangle\langle 2m1\lambda|1\mu\rangle I_E^2], \tag{6}$$

$$I_E^0 = \int u^*(^3P_J{:}pr)u(r)r\,dr, \quad I_E^2 = \int u^*(^3P_J{:}r)w(r)r\,dr, \tag{7}$$

where $u(r)$ and $w(r)$ are the radial deuteron s and d waves, respectively, and p is the proton momentum in the center of mass system.

The normalization factor N in Eqs. (5) and (6) reads

$$N^2 = \frac{2\alpha\pi k}{p^2}. \tag{8}$$

The total cross section is related to the amplitudes T_λ as

$$\sigma^{\gamma D\to np} = \frac{Mp}{12\pi}\sum_{\lambda M_i}[\overline{|T_\lambda(M1)|^2} + \overline{|T_\lambda(E1)|^2}], \tag{9}$$

$$\overline{|T_\lambda|^2} = \frac{1}{4\pi}\int d\Omega_p |T_\lambda|^2, \tag{10}$$

where M_i is the deuteron spin projection and

$$\frac{1}{2N^2}\sum_{\lambda M_i}\overline{|T_\lambda(M1)|^2} = \left(\frac{\mu_v}{M}\right)^2 |I_M^0|^2,$$

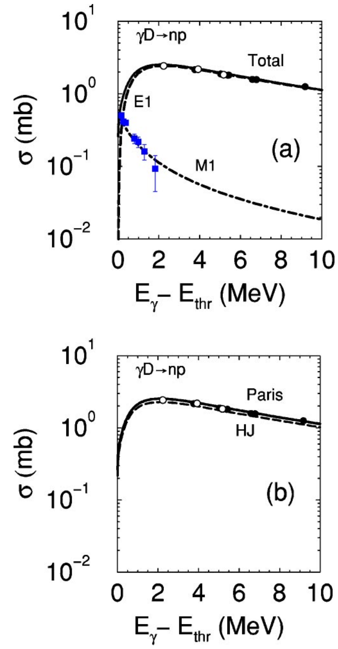

FIG. 1. (Color online) The total cross section of the deuteron photodisintegration as a function of the energy excess $\Delta E_\gamma = E_\gamma - E_{\rm thr}$. (a) Result for the Paris potential. Contributions of the $M1$ and $E1$ transitions are shown by the dashed and dot-dashed curves, respectively. (b) The total cross section for the Paris (solid) and Hamada-Johnston (dashed) potentials. The experimental data on the total cross section are taken from Refs. [38] (open circles) and [39] (filled circles). The data on $M1$-transition (filled squares) are taken from Ref. [40].

$$\frac{1}{2N^2}\sum_{\lambda M_i}\overline{|T_\lambda(E1)|^2} = |I_E^0|^2 + \frac{2}{5}|I_E^2|^2. \tag{11}$$

In the following, we will assume the average of Eq. (10) in all the quadratic forms of $T_a T_b^*$ which define the observables in the case where the angular distribution of the final nucleon is not fixed and skip the symbol "overline," for simplicity.

The wave functions for the deuteron bound state and the np scattering states are calculated using the realistic nucleon-nucleon potentials in two extreme cases: potential with a soft short-range repulsive core (Paris potential [33,34]) and potential with a hard repulsive core (HJ potential [35]).

Figure 1 shows the comparison of the available experimental data [38,39] and the result of the present calculation for the total cross section of the $\gamma D \to np$ reaction as a function of the energy excess $\Delta E_\gamma = E_\gamma - E_{\rm thr}$, where $E_{\rm thr}$ is the threshold energy $E_{\rm thr} = \epsilon(1+\epsilon/2(M_p+M_n-\epsilon)) \simeq \epsilon$ and $\epsilon = 2.23$ MeV is the deuteron binding energy. The result for the Paris potential is shown in Fig. 1(a), where each contribution from the $M1$ and $E1$ transitions is also displayed. The difference between the Paris and HJ potentials in the total cross section does not exceed 5% and disappears at $\Delta E_\gamma \to 0$ [see Fig. 1(b)] because the main contribution into the radial integrals of Eqs. (1) and (2) at low ΔE_γ comes from the relatively large distances with $r \gg 1$ fm, where the np wave functions calculated for all the realistic potentials are close to each other. This result is in agreement with those of the

TABLE I. Weak coupling constants determined from the best value of Ref. [3]. All values are given in units of 10^{-6}.

h_ρ^0	h_ρ^1	$h_\rho^{1\prime}$	h_ρ^2	h_ω^0	h_ω^1	h_π
−1.14	−0.02	−0.07	−0.95	−0.19	−0.11	0.46

previous calculations performed with various realistic potentials (see Ref. [39] for references and quotations).

III. PNC INTERACTION AND PARITY ODD ADMIXTURES

The short-range PNC potential is expressed in terms of ρ, ω, and π exchanges, and has the following form [3,41]:

$$
\begin{aligned}
V_{\rm PNC} = \frac{2ig_\rho}{M}\Bigg\{\Bigg[& h_\rho^0 \boldsymbol{\tau}_1\boldsymbol{\tau}_2 + \frac{1}{2}h_\rho^1(\tau_1^z+\tau_2^z) + \frac{1}{2\sqrt{6}}h_\rho^2(3\tau_1^z\tau_2^z \\
& - \boldsymbol{\tau}_1\cdot\boldsymbol{\tau}_2)\Bigg] \times [\boldsymbol{\Sigma}\{\boldsymbol{\nabla}, f_\rho(r)\} + (1+\chi_\rho)\boldsymbol{\Omega}\,\nabla\, f_\rho(r)] \\
& - \frac{1}{2}h_\rho^1(\tau_1^z-\tau_2^z)\mathbf{S}\{\boldsymbol{\nabla}, f_\rho(r)\} + ih_\rho^{1\prime}\left[\frac{\boldsymbol{\tau}_1\times\boldsymbol{\tau}_2}{2}\right]^z \mathbf{S}\,\boldsymbol{\nabla}\, f_\rho(r)\Bigg\} \\
& + \frac{2ig_\omega}{M}\Bigg\{\left[h_\omega^0 + \frac{1}{2}h_\omega^1(\tau_1^z+\tau_2^z)\right][\boldsymbol{\Sigma}\{\boldsymbol{\nabla}, f_\omega(r)\} \\
& + (1+\chi_\omega)\boldsymbol{\Omega}\,\boldsymbol{\nabla}\, f_\omega(r)] + \frac{1}{2}h_\omega^1(\tau_1^z-\tau_2^z)\mathbf{S}\{\boldsymbol{\nabla}, f_\omega(r)\}\Bigg\} \\
& + \frac{2g_\pi h_\pi}{\sqrt{2}M}\left\{\left[\frac{\boldsymbol{\tau}_1\times\boldsymbol{\tau}_2}{2}\right]^z \mathbf{S}\,\boldsymbol{\nabla}\, h_\pi(r)\right\},
\end{aligned}
\tag{12}
$$

where

$$
f_\omega(r) \simeq f_\rho(r) = \frac{e^{-m_\rho r}}{4\pi r}, \quad f_\pi(r) = \frac{e^{-m_\pi r}}{4\pi r}, \quad \boldsymbol{\Omega} = \frac{i}{2}[\boldsymbol{\sigma}_1\times\boldsymbol{\sigma}_2].
\tag{13}
$$

For the strong nucleon-meson coupling constants g_i and χ_i, we use commonly accepted values [9] $g_\rho=2.79, g_\omega=8.37, g_\pi=13.45$, $\chi_\rho=3.71$, and $\chi_\omega=-0.12$. The PNC meson-nucleon coupling constants h_i are taken as the best value of Ref. [3] (in the Weinberg-Salam model). The sensitivity of the observables to h_π will be discussed separately. For convenience, Table I shows all the parameters used in the present work. Odd-parity admixture states $\widetilde{\psi}$ to the deuteron wave functions and np-scattering states are defined in the first order of perturbation theory in terms of Schrödinger equation

$$
[E - H_{\rm PC}]\widetilde{\psi} = V_{\rm PNC}\psi,
\tag{14}
$$

where $H_{\rm PC}$ is the parity-conserving Hamiltonian and $V_{\rm PNC}$ is the parity-violating two-body potential. For the odd-parity $^1P_1$ admixture in a deuteron with $I=0$, we have the following expression:

$$
\widetilde{\psi}(^1P_1) = i\frac{\widetilde{u}(^1P:r)}{r}Y_{1M_i}(\hat{\mathbf{r}})\chi_{00},
$$

$$
\begin{aligned}
\widetilde{u}(^1P_1:r) = \sum_{i=\omega,\rho}\frac{2g_i\hat{h}_i^0}{\sqrt{3}}\int dr' g_1^{00}(-\epsilon;r,r')\Bigg\{\Bigg[& -\chi_i f_i'(r') \\
& + 2f_i(r')\left(\frac{\partial}{\partial r'} - \frac{1}{r'}\right)\Bigg]u(r') - \sqrt{2}\Bigg[-\chi_i f_i'(r') \\
& + 2f_i(r')\left(\frac{\partial}{\partial r'} + \frac{2}{r'}\right)\Bigg]w(r')\Bigg\},
\end{aligned}
$$

$$
\hat{h}_\rho^0 = -3h_\rho^0, \quad \hat{h}_\omega^0 = h_\omega^0,
\tag{15}
$$

where χ_{SS_z} is the two nucleon spin function, $g_l^{IS}(E;r,r')$ is the Green function of the radial Schödinger equation for the np system with the orbital momentum $l=1$, isospin $I=0$, spin $S=0$, and the energy $E=-\epsilon$.

The odd-parity $^3P_1$ admixture with $I=1$ is dominated by the π-meson-exchange weak interaction. Nevertheless, for completeness we also include the contributions of the ρ- and ω-meson exchanges for the $\Delta I=1$ transition. The net expression for the $^3P_1$ admixture reads

$$
\widetilde{\psi}(^3P_1) = i\sum_{\mu\sigma}\langle 1\mu 1\sigma|1M_i\rangle\frac{\widetilde{u}(^3P:r)}{r}Y_{1\mu}(\hat{\mathbf{r}})\chi_{1\sigma},
$$

$$
\begin{aligned}
\widetilde{u}(^3P_1:r) = \frac{2}{\sqrt{3}}\int dr' g_1^{01}(-\epsilon;r,r')\Bigg(& [g_\pi h_\pi f_\pi'(r') \\
& - \sqrt{2}g_\rho h_\rho'^1 f_\rho'(r')]\left[u(r') + \frac{1}{\sqrt{2}}w(r')\right] - \sqrt{2}(g_\omega h_\omega^1 \\
& - g_\rho h_\rho^1)\Bigg\{\left[f_\rho'(r') + 2f_\rho(r')\left(\frac{\partial}{\partial r'} - \frac{1}{r'}\right)\right]u(r') \\
& + \frac{1}{\sqrt{2}}\left\{f_\rho'(r') + 2f_\rho(r')\left(\frac{\partial}{\partial r'} + \frac{2}{r'}\right)\right]\omega(r')\Bigg\}\Bigg).
\end{aligned}
\tag{16}
$$

Figure 2(a) shows the odd-parity $^1P_1$ and $^3P_1$ admixture in the deuteron wave function for the Paris (solid curves) and HJ (dashed curves) potentials. The main difference between the two potentials appears at short distances. In case of the HJ potential, all wave functions vanish in the core region at $r \leqslant r_{\rm core}$ ($r_{\rm core}=0.48$ fm). This results in a sizable suppression of $^1P_1$ admixture because the "form factors" $f_v(r)$ in Eq. (15) decrease sharply with r. The function $f_\pi(r)$ decreases more slowly. Therefore, the $^3P_1$ admixture is not so sensitive to the choice of the potential model.

Analysis of the odd-parity component in the continuum np states shows that at $E_\gamma < 10$ MeV, the dominant contribution to the considered asymmetries comes from the $^3P_0$ admixture to the $^1S_0$ state, from the $^1S_0$ admixture to the $^3P_0$ state, and from the $^3S_1$ and $^3D_1$ components of the $^3P_1$ state. They are defined as follows:

$$
\widetilde{\psi}(^3P_0) = i\frac{\sqrt{4\pi}}{3}\sum_\mu\frac{\widetilde{u}(^3P_0:pr)}{pr}(-1)^{\mu+1}Y_{1\mu}(\hat{\mathbf{r}})\chi_{1-\mu},
\tag{17}
$$

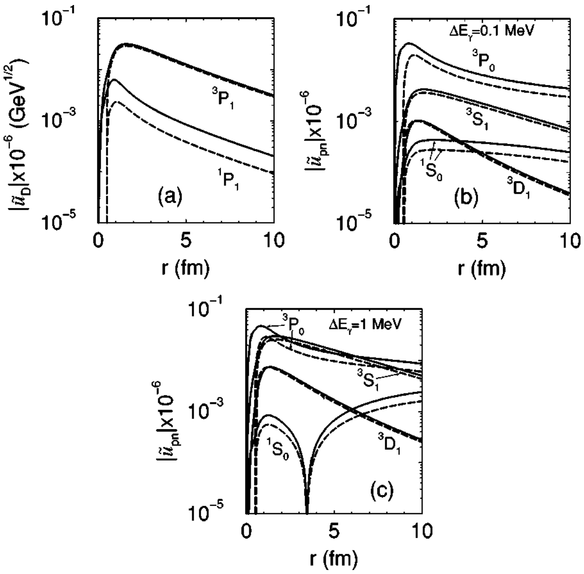

FIG. 2. The odd-parity admixture to the proton-neutron wave functions calculated with the Paris (solid curves) and HJ (dashed curves) potentials. (a) Results for the deuteron wave functions. (b) and (c) Results for the continuum np wave functions at $\Delta E_\gamma=0.1$ and 1 MeV, respectively.

$$\tilde{u}(^3P_0:pr) = -\sum_{i=\rho,\omega}\sqrt{12}g_i\hat{h}_i\int dr' g_1^{11}(E;r,r') \times\left[(2+\chi_i)f_i'(r') + 2f_i(r')\left(\frac{\partial}{\partial r'} - \frac{1}{r'}\right)\right] \times u(^1S_0:pr'),$$

$$\tilde{\psi}(^1S_0) = i\sqrt{\frac{4\pi}{3}}\frac{\tilde{u}(^1S_0:pr)}{pr}\chi_{00}\sum_m Y_{1m}^*(\hat{\mathbf{p}}), \qquad (18)$$

$$\tilde{u}(^1S_0:pr) = \sum_{i=\rho,\omega}\frac{2g_i\hat{h}_i}{\sqrt{3}}\int dr' g_0^{10}(E;r,r')\left[\chi_i f_v'(r') - 2f_i(r')\left(\frac{\partial}{\partial r'} + \frac{1}{r'}\right)\right]u(^3P_0:pr'),$$

$$\tilde{\psi}(^3S_1) = i\sqrt{4\pi}\frac{\tilde{u}(^3S_1:pr)}{pr}\chi_{1M_f}\sum_m Y_{1m}^*(\hat{\mathbf{p}}), \qquad (19)$$

$$\tilde{u}(^3S_1:pr) = -\frac{2}{\sqrt{3}}\int dr' g_0^{01}(E;r,r')\Big\{g_\pi h_\pi f_\pi'(r') - \sqrt{2}g_\rho h_\rho'^1 f_\rho'(r') + \sqrt{2}(g_\omega h_\omega^1 - g_\rho h_\rho^1) \times\left[f_\rho'(r') + 2f_\rho(r')\left(\frac{\partial}{\partial r'} + \frac{1}{r'}\right)\right]\Big\}u(^3P_1:pr'),$$

$$\tilde{\psi}(^3D_1) = i4\pi\frac{\tilde{u}(^3D_1:pr)}{pr}\sum_{\mu\sigma}\langle 2\mu 1\sigma|1M_f\rangle Y_{2\mu}(r)\chi_{1\sigma}\sum_m Y_{1m}^*(\hat{\mathbf{p}}),$$

$$\tilde{u}(^3D_1:pr) = -\sqrt{\frac{2}{3}}\int dr' g_2^{01}(E;r,r')\Big\{g_\pi h_\pi f_\pi'(r') - \sqrt{2}g_\rho h_\rho'^1 f_\rho'(r') + \sqrt{2}(g_\omega h_\omega^1 - g_\rho h_\rho^1) \times\left[f_\rho'(r') + 2f_\rho(r')\left(\frac{\partial}{\partial r'} - \frac{2}{r'}\right)\right]\Big\}u(^3P_1:pr'),$$

$$\hat{h}_\rho = h_\rho^0 - \sqrt{\frac{2}{3}}h_\rho^2, \quad \hat{h}_\omega = h_\omega^0, \qquad (20)$$

where $E=p^2/M$. The Green functions $g(E;r,r')$ in Eqs. (15)–(18) are expressed through the regular and irregular solutions of the corresponding Schrödinger equations in the standard way. For the $^3S_1$ and $^3D_1$ states, we use the spectral representation

$$Mg_l^{01}(E;r,r') = \frac{u_l(r)u_l(r')}{E+\epsilon} + \frac{2}{\pi}\int dk\frac{u(^3K_1:kr)u(^3K_1:kr')}{E-E_{\mathbf{k}}}, \qquad (21)$$

with $\int u_l^2\, dr=1$, $K=S,D$, and $E_k=k^2/M$, and keeping only the first term, because the second term does not contribute to the $M1$ transition. In this sense, our $^3S_1$, $^3D_1$ odd-parity admixtures are the only part of the corresponding total wave functions which contribute to the PNC $M1$ transition.

Figure 2(b) shows the odd-parity $^3P_0$, $^1S_0$, $^3S_1$, and $^3D_1$ admixtures for two potentials at $\Delta E_\gamma=0.1$ MeV. The $^3D_1$ function is scaled additionally by $\sqrt{P_D}$, where P_D is the D-state probability in a deuteron, because the corresponding $M1$ transition is suppressed by this factor ($P_D^{\mathrm{Paris}}=0.0577, P_D^{\mathrm{HJ}}=0.0697$). Again, one can see that in case of hard-core potentials, all wave functions vanish in the core region, which leads to the relative suppression of the odd-parity $^3P_0$ and $^1S_0$ components, whereas the $^3S_1$ and $^3D_1$ configurations defined mainly by the long-range πNN interaction are not sensitive to the potential at $r>r_{\mathrm{core}}$. In Fig. 2(c), we show the continuum wave functions at $\Delta E_\gamma=1$ MeV. The main difference as compared with the previous case appears in the $^1S_0$ odd-parity admixture. It oscillates with r more strongly and has a node at $r\simeq3.5$ fm and at $\Delta E_\gamma\simeq1$ MeV. This oscillating behavior is manifested in the corresponding $M1$ transition.

IV. ASYMMETRIES

The asymmetry of the deuteron disintegration in reaction with circularly polarized photon beam,

$$A_{RL} = \frac{\sigma_{\lambda=1} - \sigma_{\lambda=-1}}{\sigma_{\lambda=1} + \sigma_{\lambda=-1}}, \qquad (22)$$

consists of seven terms

$$A_{RL} = \sum_{i=1}^{4} V_i^\gamma + \sum_{j=1}^{3}\pi_j^\gamma, \qquad (23)$$

defined by the interplay of dipole transitions caused by the parity-conserved and parity nonconserved interaction as follows:

$$V_1^\gamma = 2\mathrm{Re}[T^*(M1{:}D \to {}^1S_0)T(E1{:}D \to {}^3\widetilde{P}_0)]/\mathcal{N}, \quad (24a)$$

$$V_2^\gamma = 2\mathrm{Re}[T^*(M1{:}D \to {}^1S_0)T(E1{:}{}^1\widetilde{P}_1 \to {}^1S_0)]/\mathcal{N}, \quad (24b)$$

$$V_3^\gamma = 2\mathrm{Re}[T^*(E1{:}D \to {}^3P_0)T(M1{:}D \to {}^1\widetilde{S}_0)]/\mathcal{N}, \quad (24c)$$

$$V_4^\gamma = 2\mathrm{Re}[T^*(E1{:}D \to {}^3P_J)T(M1{:}{}^1\widetilde{P}_1 \to {}^3P_J)]/\mathcal{N}, \quad (24d)$$

$$\pi_1^\gamma = 2\mathrm{Re}[T^*(E1{:}D \to {}^3P_J)T(M1{:}{}^3\widetilde{P}_1 \to {}^3P_J)]/\mathcal{N}, \quad (24e)$$

$$\pi_2^\gamma = 2\mathrm{Re}[T^*(E1{:}D \to {}^3P_1)T(M1{:}D \to {}^3\widetilde{S}_1)]/\mathcal{N}, \quad (24f)$$

$$\pi_3^\gamma = 2\mathrm{Re}[T^*(E1{:}D \to {}^3P_1)T(M1{:}D \to {}^3\widetilde{D}_1)]/\mathcal{N}, \quad (24g)$$

$$\mathcal{N} = \frac{1}{2N^2}\mathrm{Tr}[TT^*].$$

The explicit forms in terms of the radial integrals read

$$V_1^\gamma = -\frac{2}{3\sqrt{3}}\frac{1}{\mathcal{N}}\frac{\mu_v}{M}\mathrm{Re}\left[I_M^{0*}\int dr\, r\widetilde{u}^*({}^3P_0{:}pr)[u(r) - \sqrt{2}w(r)]\right], \quad (25a)$$

$$V_2^\gamma = -\frac{2}{\sqrt{3}}\frac{1}{\mathcal{N}}\frac{\mu_v}{M}\mathrm{Re}\left[I_M^{0*}\int dr\, ru^*({}^1S_1{:}pr)\widetilde{u}({}^1P_1{:}r)\right], \quad (25b)$$

$$V_3^\gamma = \frac{2}{3\sqrt{3}}\frac{1}{\mathcal{N}}\frac{\mu_v}{M}\mathrm{Re}\left[(I_E^{0*} - \sqrt{2}I_E^{2*})\int dr\widetilde{u}^*({}^1S_0{:}pr)u(r)\right], \quad (25c)$$

$$V_4^\gamma = \frac{2}{\sqrt{3}}\frac{1}{\mathcal{N}}\frac{\mu_v}{M}\mathrm{Re}\left[(I_E^{0*} - \sqrt{2}I_E^{2*})\int dru^*({}^3P_J{:}pr)\widetilde{u}({}^1P_1{:}r)\right], \quad (25d)$$

$$\pi_1^\gamma = -\sqrt{\frac{8}{3}}\frac{1}{\mathcal{N}}\frac{\mu_s}{M}\mathrm{Re}\left[\left(I_E^{0*} + \frac{1}{\sqrt{2}}I_E^{2*}\right)\times\int dru^*({}^3P_J{:}pr)\widetilde{u}({}^3P_1{:}r)\right], \quad (25e)$$

$$\pi_2^\gamma = \sqrt{\frac{8}{3}}\frac{1}{\mathcal{N}}\frac{\mu_s}{M}\mathrm{Re}\left[\left(I_E^{0*} + \frac{1}{\sqrt{2}}I_E^{2*}\right)\int dr\widetilde{u}^*({}^3S_1{:}pr)u(r)\right], \quad (25f)$$

$$\pi_3^\gamma = -\sqrt{\frac{2}{3}}\frac{1}{\mathcal{N}}\frac{\mu_s - 3/2}{M}\mathrm{Re}\left[\left(I_E^{0*} + \frac{1}{\sqrt{2}}I_E^{2*}\right)\times\int dr\widetilde{u}^*({}^3D_1{:}pr)w(r)\right]. \quad (25g)$$

Another asymmetry is related to the deuteron disintegration with unpolarized photon and polarized deuteron:

$$A_D = \frac{\sigma_{M_D=1} - \sigma_{M_D=-1}}{\sigma_{M_D=1} + \sigma_{M_D=-1}}, \quad (26)$$

where $M_D=1(-1)$ corresponds to the deuteron spin projection parallel (antiparallel) to the direction of the beam momentum. This asymmetry has also seven components

$$A_D = \sum_{i=1}^{4} V_i^D + \sum_{j=1}^{3}\pi_j^D. \quad (27)$$

Three of them, $V_{1,2,3}^D$, are equal with the opposite sign to the corresponding V^γ asymmetries

$$V_1^D = -V_1^\gamma, \quad V_2^D = -V_2^\gamma, \quad V_3^D = -V_3^\gamma. \quad (28)$$

In these cases, the spin of the final states is zero and the corresponding $M1$ transitions are proportional to $\delta_{-\lambda M_D}$. The other four asymmetries are expressed as

$$V_4^D = \frac{2}{\sqrt{3}}\frac{1}{\mathcal{N}}\frac{\mu_v}{M}\mathrm{Re}\left[(I_E^{0*} - \sqrt{2}I_E^{2*})\int dru^*({}^3P_J{:}pr)\widetilde{u}({}^1P_1{:}r)\right],$$

$$\pi_1^D = -\sqrt{\frac{2}{3}}\frac{1}{\mathcal{N}}\mathrm{Re}\left[\left(\frac{\mu_s - 1}{M}I_E^{0*} - \sqrt{2}\frac{\mu_s - 1/4}{M}I_E^{2*}\right)\times\int dru^*({}^3P_J{:}pr)\widetilde{u}({}^3P_1{:}r)\right],$$

$$\pi_2^D = -\frac{1}{2}\pi_2^\gamma, \quad \pi_3^D = -\frac{1}{2}\pi_3^\gamma. \quad (29)$$

The most important is the modification of π_1^D. As we will see later, the spin transitions in π_1 and π_2 proportional to μ_s are almost canceled in A_γ, but not in A_D. Therefore, the PNC weak interaction of the π exchange may be clearly manifested only in the A_D asymmetry.

V. RESULTS AND DISCUSSION

We first discuss the A_γ asymmetry. At $E_\gamma \to E_{\mathrm{thr}}$, the V_1 and V_2 terms only contribute to the total asymmetry. The signs of them are opposite and therefore their interference is destructive. The sign of the total asymmetry is defined by the dominant term. The strength of $V_{1,2}$ is determined by the values of the corresponding PNC weak coupling constants and the behavior of the proton-neutron wave function at short distances. When the functions $u(r)$ and $u({}^1S_0{:}pr)$ are smooth at $r \lesssim 1$ fm (e.g., in the zero-range approximation), one can neglect derivatives u' in Eqs. (15) and (17). Using the approximate expression for the Green function for $r' < r$

and $E\sim 0$: $g_1(E:r,r')\simeq -r'^2\theta(r-r')/3r$, neglecting w and w', and taking into account the fact that the main contribution to the odd-parity admixtures $\tilde{u}(^1P_1:r)$ and $\tilde{u}(^3P_0:pr)$ comes from the terms proportional to $f_v'(r')$, one gets the following estimate:

$$\frac{V_1^\gamma}{V_2^\gamma} \simeq -\frac{\left(h_\rho^0 - \sqrt{\frac{2}{3}}h_\rho^2\right)(2+\chi_\rho) + h_\omega^0(2+\chi_\omega)}{3h_\rho^0\chi_\rho - h_\omega^0\chi_\omega} \simeq -0.18. \tag{30}$$

This estimation coincides with the result of the plane-wave Born approximation given in Ref. [2] and shows the dominance of the $^3S_1\to{}^1\tilde{P}_1$ PNC transition with $\Delta I=0$ compared to the $^1S_0\to{}^3\tilde{P}_0$ transition with $\Delta I=0,2$. In case of the realistic NN potential, the radial np wave functions increase rapidly from zero at $r=0$ (for the hard-core potential from $r=r_{\rm core}$) to the finite value at $r\simeq 1$ fm. Since f_v and $|f_v'|$ decrease with r, the dominant contribution to the integrals in Eqs. (15) and (17) comes from the region at $r=0.6$–1.2 fm. This leads to increase of $|V_1^\gamma/V_2^\gamma|$ and to decrease of the asymmetries $|A_{RL}|$ and $|A_D|$. Of course, we cannot neglect the terms with derivatives u' because they are essential just in the region of the dominant contribution of the corresponding integrals. In our case $u'(r), w'(r), u'(^1S_0:r)$ at $r\lesssim 1.2$ fm are positive and large, especially for the hard-core HJ potentials. In Eq. (15), the term proportional to $u'(r)$ gives a constructive contribution and enhance $|V_2|$, whereas in Eq. (17), $u'_{np}(pr)$ contributes destructively and suppresses $|V_1|$. As a result, we get the ratio of V_1^γ/V_2^γ close to the estimate of Eq. (30).

Figure 3(a) shows the asymmetries A_{RL} as a function of ΔE_γ together with the partial asymmetries V_i and π_i. When ΔE_γ increases, the PNC $M1$ transitions become important. At low ΔE_γ, the asymmetries V_3^γ caused by the $\Delta I=0,2$ PNC forces, and V_4^γ generated by $\Delta I=0$ forces are close to each other numerically with the same sign. However, at $\Delta E_\gamma \sim 0.5$ MeV, V_3^γ decreases, changes sign, and then its absolute value becomes much smaller than $|V_4^\gamma|$, and it does not affect the total asymmetry. In the limit of $\Delta E_\gamma\to 0$, the present result of $A_{LR}=3.35\times 10^{-8}$ is in agreement with the previous calculations for the circular photon polarization in the $np\to D\gamma$ reaction **(**$P_\gamma=(1.8$–$5.6)\times 10^{-8}$ [17–19]**)**.

The PNC transitions with $\Delta I=1$ ($\Delta S=0$) are described by the π_1^γ, π_2^γ, and π_3^γ terms, where $\pi_{1,2}^\gamma$ terms are dominant and they are mostly determined by the weak π-meson-exchange interaction. In Fig. 3(a), we show the π_1^γ asymmetry, the sum of $\pi_2^\gamma+\pi_3^\gamma$-terms, and the coherent sum of all the $\Delta I=1$ transitions denoted as π^γ. At $\Delta E\sim 10$ MeV, the absolute values of π_1^γ and π_2^γ are the biggest among the other (V_i) terms and close to each other. But their signs are opposite. Therefore, the coherent sum is rather small:

$$\pi_{12}^\gamma = \pi_1^\gamma + \pi_2^\gamma \sim \mu_s(\tilde{I}_M^1 - \tilde{I}_M^2) \sim \mu_s O(P_D), \tag{31}$$

where $\tilde{I}_M^1$ and $\tilde{I}_M^2$ are the radial integrals for the $M1$ transitions in Eqs. (25e) and (25f), respectively. The finite value of π_{12}^γ is mainly caused by the nonsymmetrical contribution of

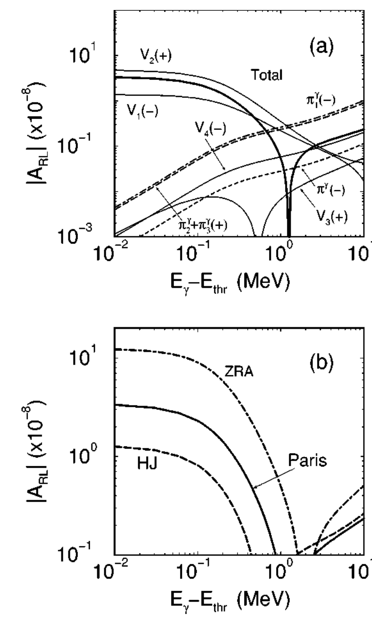

FIG. 3. Asymmetry of the deuteron disintegration in the reaction $\gamma D\to pn$ with circular polarized photon and unpolarized deuteron as a function of the energy excess $E_\gamma - E_{\rm thr}$. (a) Relative contribution of the different odd-parity transitions for the Paris potential. The sign in the bracket denotes the sign of the corresponding term. (b) Comparison of the total asymmetry for the Paris (solid), Hamada-Johnston (dashed) potentials, and the modified ZRA of Ref. [29] (dot-dashed).

the deuteron d wave in π_1^γ, and π_2^γ and it almost vanishes when $P_D=0$. In case of the zero-range approximation (ZRA) in the limit $\Delta E_\gamma\to 0$, this cancellation is exact [29]. In the real case the total contribution of the $\Delta I=1$ PNC interaction (π^γ) is finite. However, its absolute value is smaller by a factor of 27 than the result of Ref. [28]. Therefore, it seems to be difficult to get information about the $\Delta I=1$ PNC forces from A_{RL}^γ.

The coherent interference of the V_1^γ, V_2^γ, and V_4^γ terms leads to a sharp decrease of A_{RL} down to zero at $\Delta E_\gamma \simeq 1.3$ MeV (in case of the Paris potential), and a change of sign from positive to negative. Figure 3(b) shows the total asymmetry A_{RL} for the two potentials. For illustration, we also show the prediction of Ref. [29] for the modified ZRA model. One can see that the behavior of the asymmetry A_{RL} is similar qualitatively for the quite different models. In case of the HJ potential, the asymmetry is smaller. The difference between two potentials at low photon energy $\Delta E_\gamma = 0.01$–1 MeV amounts to a factor of 2.5–3. The intercept $A_{RL}=0$ is shifted towards lower energies. The prediction of the modified ZRA model [29] is close qualitatively to those of the Paris potential but the absolute value of A_{RL} is much greater and the position of the intercept is shifted towards higher energies. This comparison with the HJ potential and the modified ZRA model has a rather illustrative character because the realistic potentials with a soft repulsive core are commonly accepted for more adequate description of the short-range phenomena. From this point of view, only the prediction obtained with the Paris potential seems to be realistic.

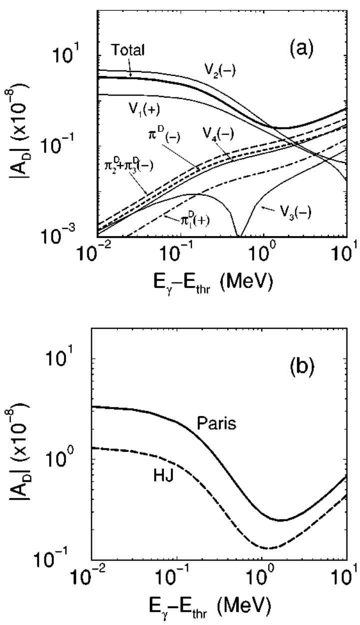

FIG. 4. Asymmetry of the deuteron disintegration in the $\gamma D \rightarrow pn$ reaction with polarized deuteron and unpolarized photon as a function of the energy excess $E_\gamma - E_{\rm thr}$. (a) Relative contribution of different odd-parity transitions for the Paris potential. Notation is the same as in Fig. 3(a). (b) Comparison of the asymmetry for the Paris and Hamada-Johnston potentials.

Figure 4(a) shows the A_D asymmetry as a function of ΔE_γ. There are two main differences compared to the A_{RL} asymmetry. First, the components V_2 and V_4 are of the same sign. Second, there is no cancellation between the ${}^3\widetilde{P}_1 \rightarrow {}^3P_J$ and $D \rightarrow {}^3\widetilde{S}_1$ transitions. Their coherent sum now behaves as

$$\pi_{12}^D = \pi_1^D + \pi_2^D \sim \left(\mu_s - \frac{1}{2}\right)\widetilde{I}_M^1, \qquad (32)$$

and becomes a significant part of the asymmetry at large ΔE_γ. The sum of all transitions generated by the $\Delta I = 1$ PNC forces $\pi^D = \pi_{12}^D + \pi_3^D$ has the same sign as the V_2 and V_4 components. This leads to a nonmonotonical behavior of $|A_D|$ with a local minimum at $\Delta E_\gamma \simeq 2$ MeV, but the sign of A_D remains to be the same at $0 < \Delta E_\gamma \leqslant 10$ MeV and negative. In Fig. 4(b), we compare the results for A_D calculated with the two potentials. The difference between the two asymmetries decreases with the increasing photon energy, however, the two results are similar in shape.

The weak π-meson exchange is mostly important at large ΔE_γ. For illustration, Fig. 5 shows the asymmetry A_D calculated as a function of ΔE_γ at different values of h_π which cover its theoretical uncertainty: $0 \leqslant h_\pi \leqslant 2.5 h_\pi^{\rm best}$, where $h_\pi^{\rm best}$ is the best value of DDH. One can see that the constructive interference between weak π and vector meson-exchange results in increasing the absolute value of A_D with increasing h_π, and leads to a shift in the position of the local minimum towards the lower energies. The absolute value of $|A_D|$ increases by a factor of 3 when R_π changes from 0 to 2.5 at $1 \lesssim \Delta E_\gamma \lesssim 10$ MeV.

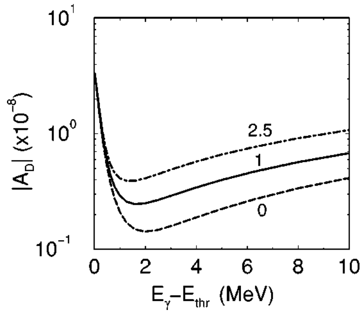

FIG. 5. Asymmetry of the deuteron disintegration in the $\gamma D \rightarrow pn$ reaction (A_D) with different values of the PNC π-exchange coupling constant $R = h_\pi / h_\pi^{\rm best} = 0, 1, 2.5$, where $h_\pi^{\rm best}$ is the best value of Ref. [3].

Using the energy dependence of A_{RL} and A_D, one can obtain the relations between the weak coupling constants. Thus, the standard representations of asymmetries through h_i are

$$A_{RL} = a_\rho^0 g_\rho h_\rho^0 + a_\rho^2 g_\rho h_\rho^2 + a_\omega^0 g_\omega h_\omega^0 + a_v^1 (g_\omega h_\omega^1 - g_\rho h_\rho^1) + a_\rho'^1 g_\rho h_\rho'^1 + a_\pi g_\pi h_\pi, \qquad (33)$$

$$A_D = b_\rho^0 g_\rho h_\rho^0 + b_\rho^2 g_\rho h_\rho^2 + b_\omega^0 g_\omega h_\omega^0 + b_v^1 (g_\omega h_\omega^1 - g_\rho h_\rho^1) + b_\rho'^1 g_\rho h_\rho'^1 + b_\pi g_\pi h_\pi. \qquad (34)$$

In the ideal case, having the asymmetries at six energy points and using the energy dependence of a_i and b_i one extracts h_i unambiguously. In practice, the number of "independent" equations for determination of h_i is smaller, because some of a_i (b_i) are rather weak. The energy dependence of the coefficients a_i and b_i is shown in the Figs. 6(a) and 6(b), respec-

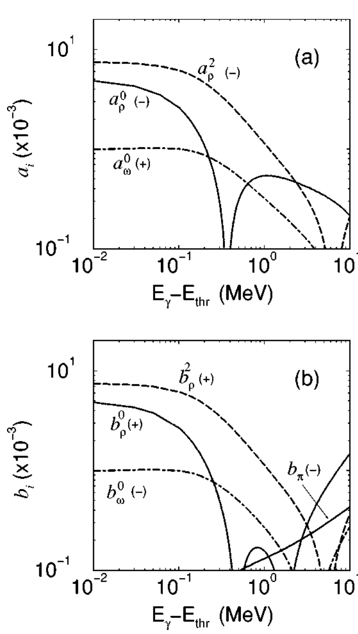

FIG. 6. (a) The quantities a_i of Eq. (35). (b) The quantities b_i of Eq. (36). Only the large components are displayed. Results are obtained with the Paris potential.

tively. For simplicity, we display only the dominant terms.

There are several points, where A_{RL} and A_D are particularly interesting. At $\Delta E \to 0$, where the absolute values of both the asymmetries have a maximum, we get the following relations:

$$A_{RL} \simeq -(4.82 g_\rho h_\rho^0 + 7.43 g_\rho h_\rho^2 - 0.99 g_\omega h_\omega^0) \times 10^{-3}, \tag{35}$$

$$A_D \simeq -A_{RL}. \tag{36}$$

The point $\Delta E \sim 10$ MeV can be used for analyzing the π-meson-exchange contribution in A_D:

$$A_D \simeq (1.46 g_\rho h_\rho^0 - 0.36 g_\rho h_\rho^2 + 0.27 g_\omega h_\omega^0 - 0.43 g_\pi h_\pi) \times 10^{-3}. \tag{37}$$

The coefficient b_π is governed by the long-range interactions and therefore is not sensitive to the model of the *NN* interaction at short distances.

The position of intercept $A_{RL}=0$ at $\Delta E_\gamma \simeq 1.3$ MeV may be also used for fixing the relation between the coupling constants, but the experiment to find this position would be very difficult. On the other hand, another relation may be obtained when one of the term in Eqs. (33) and (34) vanishes, but asymmetries have a finite and reasonable value. Thus, we have at $\Delta E_\gamma \simeq 0.4$, $a_\rho^0=0$, and therefore

$$A_{RL}(\Delta E_\gamma \simeq 0.4 \text{ MeV}) \simeq -(3.13 g_\rho h_\rho^2 - 0.67 g_\omega h_\omega^0) \times 10^{-3}. \tag{38}$$

The relations (35)–(38) are derived using the energy dependence of the coefficients a_i and b_i in Eqs. (33) and (34) shown in Fig. 6. The latter is defined by the short-range behavior of the *NN* forces, and is obtained with the Paris potential which has been, in particular, designed for the adequate description of various phenomena sensitive to the nucleon interaction at short distances. On the other hand, the Paris potential cannot describe the neutron-proton singlet scattering length which is its obvious disadvantage. Nevertheless, we are convinced that our results for the Paris potential would coincide within ~20–30 % accuracy with the predictions obtained with the other soft-core realistic potentials. This level of accuracy corresponds to the difference between the present result of $A_{RL}(E_\gamma=E_{\text{thr}})$ and the previous calculations of P_γ with different realistic potentials [18].

VI. SUMMARY

We have analyzed the energy dependence of two PNC asymmetries in the deuteron photodisintegration: one with a circularly polarized photon beam (A_{RL}) and another with a polarized deuteron target (A_D). We show that by combining the measurements of A_{RL} and A_D, valuable information on the PNC nuclear forces may be obtained; namely, using the energy dependence of A_{RL} and A_D, three constraints (equations) for determination of the PNC coupling constants will be obtained.

Finally, we stress that the present investigation is a very first step. It would be important to verify if the predicted asymmetries are universal in the framework of other realistic potentials invoking the meson-exchange currents and relativistic effects [42]. The role of the higher multipole transitions at higher energies is not quite clear.

After completing this paper, the work by Liu, Hyun, and Desplanques has appeared in Ref. [43]. The authors have analyzed the A_{RL} asymmetry using the realistic Argonne AV18 potential. In spite of some difference between our models, the results of both papers are consistent with each other. Reference [43] gives $A_{RL}(\Delta E_\gamma \simeq 0) \simeq +2.53 \times 10^{-8}$ and A_{RL} changes its sign at $\Delta E_\gamma \sim 1.5$ MeV. The contribution of the weak π-exchange transition is suppressed dynamically and it is a factor of about 30 smaller than the prediction of Ref. [28].

ACKNOWLEDGMENTS

We thank S. Date', H. Ejiri, C.-P. Liu, I. Khriplovich, and Y. Ohashi for fruitful discussion. We also thank our anonymous source for notice on the estimation of the PNC asymmetry (A_{RL}) by Schiavilla [44], who shows that the weak pion-exchange transitions are strongly suppressed and the position of the node in asymmetry depends on the choice of the potential. One of the authors (A.I.T.) thanks M. Yasuoka, the director of Advanced Science Research Center, for his hospitality to stay at SPring-8. This work was supported in part by the Japan Society for the Promotion of Science (JSPS), and was strongly stimulated by a new project to produce a high-intensity MeV γ rays by inverse Compton scattering at SPring-8.

[1] E. M. Henley, Annu. Rev. Nucl. Sci. **19**, 367 (1969).
[2] E. G. Adelberger and W. C. Haxton, Annu. Rev. Nucl. Part. Sci. **35**, 501 (1985); W. Haeberli and B. R. Holstein, in *Symmetries and Fundamental Interactions in Nuclei*, edited by W. C. Haxton and E. M. Henley (World Scientific, Singapore, 1996), p. 17.
[3] B. Desplanques, J. F. Donoghue, and B. R. Holstein, Ann. Phys. (N.Y.) **124**, 449 (1980).
[4] Ulf-G. Meißner and H. Weigel, Phys. Lett. B **447**, 1 (1999).
[5] E. M. Henley, W.-Y. P. Hwang, and L. S. Kisslinger, Phys. Lett. B **367**, 21 (1996); **440**, 449 (1998).
[6] V. M. Dubovik and S. V. Zenkin, Ann. Phys. (N.Y.) **172**, 100 (1986).
[7] G. B. Feldman, G. A. Crawford, J. Dubach, and B. R. Holstein, Phys. Rev. C **43**, 863 (1991).
[8] W. C. Haxton, C.-P. Liu, and M. J. Ramsey-Musolf, Phys. Rev. C **65**, 045502 (2002).
[9] E. G. Adelberger, M. M. Hindi, C. D. Hoyle, H. E. Swanson,

R. D. Von Lintig, and W. C. Haxton, Phys. Rev. C **27**, 2833 (1983).
[10] S. A. Page *et al.*, Phys. Rev. C **35**, 1119 (1987).
[11] C. S. Wood, S. C. Bennett, D. Cho, B. P. Masterson, J. L. Roberts, C. E. Tanner, and C. E. Wieman, Science **275**, 1759 (1997).
[12] C. S. Wood, S. C. Bennett, D. Cho, C. E. Tanner, and C. E. Wieman, Can. J. Phys. **77**, 7 (1999).
[13] V. V. Flambaum and D. W. Murray, Phys. Rev. C **56**, 1641 (1997).
[14] A. R. Berdoz *et al.*, Phys. Rev. Lett. **87**, 272301 (2001).
[15] A. R. Berdoz *et al.*, Phys. Rev. C **68**, 034004 (2003).
[16] V. A. Knya'zkov, E. A. Kolomenskii, V. M. Lobashov, V. A. Nazarenko, A. N. Pirozhkov, A. I. Shablii, E. V. Shulgina, Yu. V. Sobolev, and A. I. Yegorov, Nucl. Phys. **A417**, 209 (1984).
[17] G. S. Danilov, Phys. Lett. **35B**, 579 (1971); Sov. J. Nucl. Phys. **14**, 443 (1972).
[18] K. R. Lassey and B. H.J. McKellar, Phys. Rev. C **11**, 349 (1975); **12**, 721(E) (1975); M. Gari and J. Schlitter, Phys. Lett. **59B**, 118 (1975); J. P. Leroy, J. Micheli, and D. Pignon, Nucl. Phys. **A280**, 377 (1977).
[19] B. Desplanques, Nucl. Phys. **A335**, 147 (1980).
[20] J. F. Cavaignac, B. Vignon, and R. Wilson, Phys. Lett. **67B**, 148 (1977).
[21] B. Desplanques, Phys. Lett. B **512**, 305 (2001).
[22] M. Snow *et al.*, Nucl. Instrum. Methods Phys. Res. A **440**, 729 (2000).
[23] W.-Y. P. Hwang, E. M. Henley, Ann. Phys. (N.Y.) **129**, 47 (1980).
[24] W.-Y. P. Hwang, E. M. Henley, and G. A. Miller, Ann. Phys. (N.Y.) **137**, 378 (1981).
[25] R. Schiavilla, J. Carlson, and M. Paris, Phys. Rev. C **67**, 032501 (2003).
[26] B. Desplanques, Phys. Rep. **297**, 1 (1998).
[27] H. C. Lee, Phys. Rev. Lett. **41**, 843 (1978).
[28] T. Oka, Phys. Rev. D **27**, 523 (1983).
[29] I. B. Khriplovich and R. V. Korkin, Nucl. Phys. **A690**, 610 (2001).
[30] As is evident from Ref. [29], the idea of cancellation of the PNC $\Delta I=1$ transitions in the A_{RL} asymmetry belongs to Desplanques.
[31] U. G. Meissner, Mod. Phys. Lett. A **5**, 1703 (1990).
[32] R. V. Korkin, nucl-th/0206044.
[33] M. Lacombe, B. Loiseau, R. Vinh Mau, J. Cote, P. Pires, and R. de Tourreil, Phys. Lett. **101B**, 139 (1981).
[34] M. Lacombe, B. Loiseau, J. M. Richard, R. Vinh Mau, J. Cote, P. Pires, and R. de Tourreil, Phys. Rev. C **21**, 861 (1980).
[35] T. Hamada and I. D. Johnston, Nucl. Phys. **34**, 382 (1962).
[36] D. B. Kaplan, M. J. Savage, R. P. Springer, and M. B. Wise, Phys. Lett. B **449**, 1 (1999).
[37] M. J. Savage, R. P. Springer, Nucl. Phys. **A686**, 413 (2001).
[38] C. A. Barnes, J. H. Carver, G. H. Stafford, and D. H. Wilkinson, Phys. Rev. **86**, 359 (1952).
[39] Y. Birenbaum, S. Kahane, and R. Moreh, Phys. Rev. C **32**, 1825 (1985).
[40] W. Tornow, N. G. Czakon, C. R. Howell, A. Hutcheson, J. H. Kelley, V. N. Litvinenko, S. F. Mikhailov, I. V. Pinayev, G. J. Weisel, and H. Witala, Phys. Lett. B **574**, 8 (2003).
[41] E. M. Henley, Nucl. Phys. **A300**, 273 (1978).
[42] J. Carbonell, B. Desplanques, V. A. Karmanov, and J. F. Mathiot, Phys. Rep. **300**, 215 (1998).
[43] C.-P. Liu, C. H. Hyun, and B. Desplanques, Phys. Rev. C **69** 065502 (2004).
[44] See R. Schiavilla, http://mocha.phys.washington.edu/~int_talk/Workshops/int_03_3/People/Schiavilla_R